Environ Geol (2007) 52:409–420
DOI 10.1007/s00254-006-0589-2

ORIGINAL ARTICLE

Spatial relationships of salt distribution and related physical changes of underlying rocks on naturally weathered sandstone exposures (Bohemian Switzerland National Park, Czech Republic)

R. Přikryl · L. Melounová · Z. Vařilová · Z. Weishauptová

Received: 6 October 2006 / Accepted: 22 November 2006 / Published online: 23 December 2006

Abstract Efflorescence, case hardening, and granular disintegration represent common weathering features of Upper Cretaceous quartz sandstones exposed in the Bohemian Switzerland National Park (NW Bohemia, Czech Republic). Salt species (sulphates: gypsum ($CaSO_4{\cdot}2H_2O$), potassium alum ($KAl(SO_4)_2{\cdot}12H_2O$), tschermigite ($NH_4Al(SO_4)_2{\cdot}12H_2O$), alunite ($K(Al_3(SO_4)_2(OH)_6$), and alunogen ($Al_2(SO_4)_3{\cdot}17H_2O$), minor nitrates: nitrammite (NH_4NO_3)) determined by X-ray diffraction exhibit vertical and geographic zoning. More soluble salts (chlorides, nitrates, tschermigite) crystallize preferentially on the cliffs exposed to the south, whereas the north face is characterized by the presence of less soluble phases: gypsum and $K(Al_3(SO_4)_2(OH)_6$. Vertical zoning of salt distribution on natural outcrops differs from the salt distribution in masonry. Salt distribution near the base of the cliff (profile to about 2–2.5 m above the ground) is affected by capillary rise from the ground level (first maximum of water-soluble salts at the level of 1–1.5 m above the ground) and by percolation of precipitation through the overhanging rock sequence (second maximum of 2–2.5 m above the ground). Percolation of salt solution from higher parts is affected by the asperity of the rock surface. The concentration of salts (determined by ion exchange chromatography) correlates to the changes of physical properties: bulk porosity, microporosity and water absorption. The porosity, microporosity, moisture content and absorption generally increase with the increasing volume of sulphates and nitrates.

Keywords Sandstone weathering · Salts · Physical properties · Zoning · Czech Republic

R. Přikryl (✉) · L. Melounová
Institute of Geochemistry, Mineralogy and Mineral Resources, Faculty of Science, Charles University, Albertov 6, 128 43 Prague 2, Czech Republic
e-mail: prikryl@natur.cuni.cz

Z. Vařilová
Bohemian Switzerland National Park Administration, Pražská 52, 407 46 Krásná Lípa, Czech Republic

Z. Vařilová
Institute of Geology, Academy of Sciences of the Czech Republic, Rozvojová 269, 165 02 Praha 6, Lysolaje, Czech Republic

Z. Weishauptová
Institute of Rock Structure and Mechanics, Academy of Sciences of the Czech Republic, V Holešovičkách 41, 182 09 Prague 8, Czech Republic

Introduction

The mechanism of salt introduction into porous rocks and related deterioration of the rock physical properties is generally understood to be salt weathering (Goudie and Viles 1997; Charola 2000). This weathering process is being extensively studied primarily because of the destruction of stone monuments but also due to the development of distinct geomorphic features like honeycombs (e.g. Rodriguez-Navarro et al. 1999). Salt weathering commonly affects porous rocks like sandstones which are susceptible to the movement of water-soluble salts.

The role of salts in rock weathering has been recognised during last decades both in natural areas and on monuments. The salts act not only as a physical force but as saline solutions and also facilitate the dissolution rates of silicate minerals (Young

1987; Magee et al. 1988). The sources of salts can be found elsewhere (Price 1996)—in rock itself, in the ground, from deicing salts, sea spray, in other materials present in the masonry (Smith et al. 2001), previous restoration/intervention (Přikryl et al. 2004), due to the activity of microorganisms (Machill et al. 1997) or from the atmosphere (Camuffo et al. 1983). Sourcing of salts, namely of sulphates is possible through isotopic analysis of $\delta^{34}S$ and $\delta^{18}O$ (Cortecci and Longinelli 1970; Pye and Schiavon 1989; Torfs et al. 1997).

Previously, the study of spatial distribution of salts has focused on their occurrence in masonry and monuments (Arnold 1982; Zehnder 1993, 1996; Steiger 1996; Steiger et al. 1997; Behlen et al. 1997). The study of directional dependence (both geographic orientation and vertical zoning) of salt distribution on natural rocks exposed in a natural environment is still missing. This paper therefore focuses on the relationship between spatial distribution of salts crystallizing on natural outcrops and of related changes of physical properties of sandstones. The study also aims to compare salt distribution on natural outcrops with previously published models relevant for masonry. The contribution of other climatic factors like freeze/thaw cycling is evident for the studied area but is beyond the scope of this paper.

Study area and samples

All studied samples were collected in the area of the National Park Bohemian Switzerland (NW part of the Czech Republic, Fig. 1a) where weathering processes, tectonic forces, and geomorphic evolution were responsible for the development of rock cities (Engel and Kalvoda 2002). The area makes part of the Bohemian Cretaceous Basin, the largest sedimentary unit of Bohemian Massif formed during Upper Cretaceous. It comprises several lithologic and stratigraphic members among which quartz sandstones dominate.

Quartz sandstones (Turonian) belonging to the thick-bedded type exhibit presence of large morphological forms (plateaux, canyons, and cliffs up to 150 m high), medium size morphological forms (rock arches among which the Pravčice Rock Arch is the best known, rock ledges, chimney rocks, and shelters) and small morphological aspects (honeycombs, cavities, and/or pseudokarst karren). Macroscopically observable phenomena include surface hardening of the exposed rocks (due to the case hardening by secondary silicification and/or ferruginization of the surface), granular disintegration, and efflorescence (Vařilová 2002). Current research activity focuses on the study of sandstone weathering processes of sandstone weathering (Soukupová et al. 2002) and for long-term monitoring of rock slope stability in the area (Zvelebil et al. 2002).

The samples were taken from seven profiles that provided efflorescence and rock substrate from four geographic orientations (Fig. 1b). The surface exposed to the north represents location with no insulation and smooth vertical profile. South, east and west exposed surfaces are more undulated. The surface oriented to the south is exposed both to precipitation and to high insulation and evaporation. Similar trends can be observed also on east and west exposed surfaces.

The sampling profiles were located on the exposed sandstone cliffs (the so called Wing Wall) showing variable morphology in the vertical profile but ensuring at least 20 m of smooth vertical surface above the ground (path). The sampling profiles were oriented from the ground to a height of about 2.5 m and samples were collected in the intervals of about 0.5 m (cf. Table 1).

It should be noted that sampling was permitted by National Park Management Authority to be conducted to the minimum extent because of the location of the study area in the core of the most protected zone of the National Park. The efflorescence (a few grams for each sample) was scratched and stored in poly zip bags. The rock samples (irregular pieces up to 30 cm^3) were carefully chiselled and stored in poly zip bags as well to retain the original moisture content of the rock. All samples were collected during a dry period in early autumn, 2005.

Methods

Analysis of salt efflorescence

Salt efflorescence was analysed for phase composition by X-ray diffraction (XRD) that is the most common analytical method used for mineralogical study of salts in rock weathering studies. The XRD measurement was performed under the following conditions: diffractometer X′Pert Pro, PANalytical B.V. (laboratory of X-ray diffraction, Institute of Geochemistry, Mineralogy and Mineral Resources, Charles University in Prague), anode CuKα, generator settings 40 kV and 30 mA, degrees 2theta: 3–70°, step size 0.05°, scan step time 150 s. The XRD patterns were evaluated by X′Pert HighScore 1.0d, PANalytical B.V. software using a diffraction pattern database (JCPDS 1999).

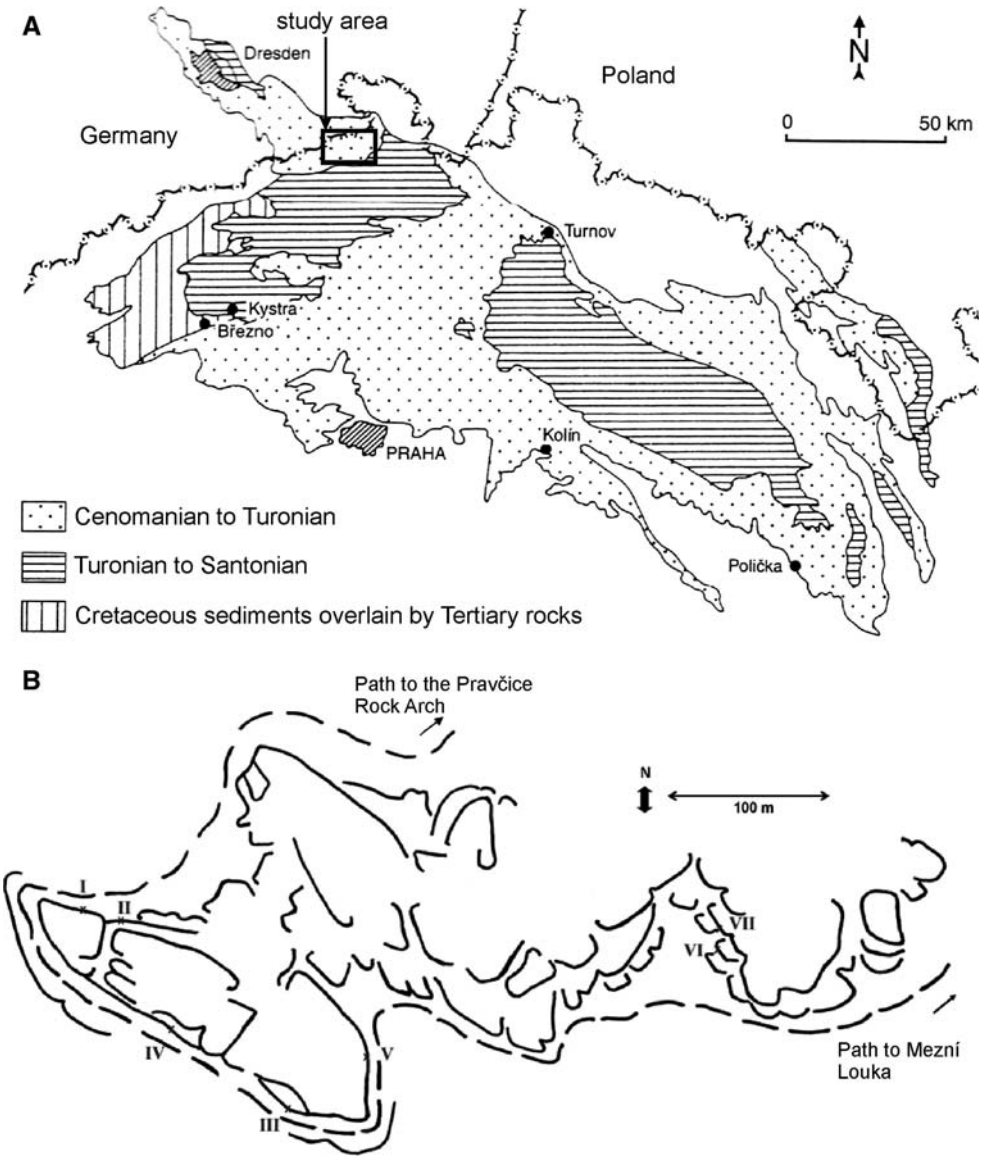

Fig. 1 Position of the studied area (**a**) and location of the sampling profiles on the Wing Walls (Křídelní stěny) cliffs

Determination of water-soluble salts

The chemical composition of water-soluble salts present in the pore system of the rock was analysed by ion exchange chromatography allowing precise determination of cations and anions (e.g., McAlister 1996). About 1 g of rock powder prepared by tender dry grinding of the surface layer of the rock (0–1 cm) was diluted in 100 ml of deionised distilled water for 12 h. The measurement was performed using Detector Shodex CD-5, Delta Chrom SDS 030 pump and Autosampler AS 100 (WATREX Praha Ltd.). The anions were determined using a column 150 × 3 mm IC Anion II 10 μm supresor, 9 mM H_2SO_4. 1 mM Na_2CO_3 and 8 mM $NaHCO_3$ were the eluents. The cations were detected by 125 × 4 mm Universal Cat 1–2 column. The eluents were 5 mM citric acid and 1 mM dipicolin acid. The following anions: Cl^-, F^-, NO_2^-, NO_3^-, PO_4^{3-}, SO_4^{2-} and cations: K^+, Na^+, NH_4^+, Ca^{2+}, Mg^{2+} were measured.

Rock petrography

The mineralogical composition and rock fabric were examined by conventional optical microscopy of thin sections (petrographic microscope LEICA DMLP, optical laboratory of the Institute of Geochemistry, Mineralogy and Mineral Resources, Charles University in Prague). The pore space was decorated by epoxy resin-fluorescent dye mixture (Nishiyama and Kusuda 1994; Přikryl 2007) before preparation of the thin section. This treatment of samples allows visualisation

Table 1 List of samples

Sample	Height above the ground (m)	Type of the sample
North facing exposure		
KS/I/1	0.5	Rock-profile I
KS/I/2	1	Rock-profile I
KS/I/3	1	Rock-profile I
KS/I/4	2	Rock-profile I
KS/I/5	2.5	Rock-profile I
KS/II/1a	0.5–0.6	Efflorescence-profile II
KS/II/2a	1–1.1	Efflorescence-profile II
KS/II/3a	2–2.2	Efflorescence-profile II
KS/II/4a	2.5–2.6	Efflorescence-profile II
South facing exposure		
KS/III/1	1.8	Rock + efflorescence
KS/IV/1	0.35	Rock-profile IV
KS/IV/2	0.7	Rock-profile IV
KS/IV/2.1		Rock-depth profile
KS/IV/2.2		
KS/IV/2.3		
KS/IV/2.4		
KS/IV/3	1.1	Rock-profile IV
KS/IV/4.1	1.6	Rock-profile IV
KS/IV/4.2	1.6	Rock-profile IV
KS/IV/5	1.9	Rock-profile IV
KS/IV/1a	0.35	Efflorescence-profile IV
KS/IV/2a	0.7	Efflorescence-profile IV
KS/IV/3a	1.1	Efflorescence-profile IV
KS/IV/4a	1.5	Efflorescence-profile IV
KS/IV/5a	1. 8–1.9	Efflorescence-profile IV
KS/IV/6a	2.1–2.2	Efflorescence-profile IV
East facing exposure		
KS/V/1	0.5	Rock-profile V
KS/V/2	1	Rock-profile V
KS/V/3	1.5	Rock-profile V
KS/V/4	2	Rock-profile V
KS/V/1a	0.4 – 0.5	Efflorescence-profile V
KS/V/2a	1 – 1.1	Efflorescence-profile V
KS/V/3a	1.4	Efflorescence-profile V
KS/V/4a	1.7	Efflorescence-profile V
KS/V/5a	1.8	Efflorescence-profile V
KS/V/6a	2.1	Efflorescence-profile V
KS/V/7a	5	Efflorescence
KS/V/8a	6	Efflorescence
KS/V/9a	6	Efflorescence
West facing exposure		
KS/VI/1	0.5	Rock-profile VI
KS/VI/2	1	Rock-profile VI
KS/VI/3	1.55	Rock-profile VI
KS/VI/4	2	Rock-profile VI
KS/VI/5	2.5	Rock-profile VI
KS/VI/1a	0.7	Efflorescence-profile VI
KS/VI/2a	1.2	Efflorescence-profile VI
KS/VI/3a	1.5–1.6	Efflorescence-profile VI
KS/VI/4a	2–2.1	Efflorescence-profile VI
KS/VI/5a	2.8	Efflorescence-profile VI
West facing exposure		
KS/VII/1	0.6–0.7	Rock-profile VII
KS/VII/1a	0.4	Efflorescence-profile VII
KS/VII/2a	0.5	Efflorescence-profile VII
KS/VII/3a	0.8	Efflorescence-profile VII
KS/VII/4a	1	Efflorescence-profile VII
KS/VII/5a	1.6	Efflorescence-profile VII
KS/VII/6a	2.1	Efflorescence-profile VII

of the pore space if the optical microscope is equipped with the source of ultraviolet light.

Physical properties and pore system analysis

Among numerous physical properties (such as density, elasticity, strength) the moisture content, bulk porosity and water absorption were determined following the conventional testing procedures (e.g. Goodman 1989; Price 1990). A more detailed study of the pore system was performed by a mercury intrusion technique that is based on the behaviour of non-wetting liquids in capillary pores (e.g., Adamson 1967). The resistance of a pore against the penetration (interface tension) can be overcome by exerting an appropriate external pressure. The range of measured pore radii rises from Washburn's equation (e.g., Adamson 1967):

$$r = -\frac{2\sigma \cos \varphi}{P},$$

where r is pore radius, σ is surface tension of mercury, Φ is mercury wetting angle of pore surface ($\Phi > 90°$) and P is absolute pressure exerted. The smallest pore radius is limited by maximum applied pressure. The largest pore evaluated by mercury intrusion is given by pressure near the atmospheric one at which the measurement starts. Each increment of pressure causes the group of smaller pores to be filled. Through this measurement, pore volume, pore radii, pore size distribution, and pore surface area can be evaluated.

In this study, the measurement was performed on a POROSIMETER 2,000 Carlo Erba (Institute of Rock Structure and Mechanics, Academy of Sciences of the Czech Republic). The operating pressure 0.1–200 MPa allows recording the pores showing effective radii 3.7–7,500 nm, corresponding to meso- and macropore groups (mm-porosity) according to IUPAC classification (see e.g., Marsh and Rodríguez-Reinoso 2000). The measured values were computed using MILESTONE 200 Carlo Erba software.

Results and discussion

Rock substrate

In the studied area, the only rock present is fine- to medium-grained quartz sandstone. The clastic component contains 93–98 vol.% of quartz (Fig. 2) and 2–7 vol.% of K-feldspars that are highly corroded and partly transformed to clay minerals. The transformation of feldspars in this area seems, however, to be an

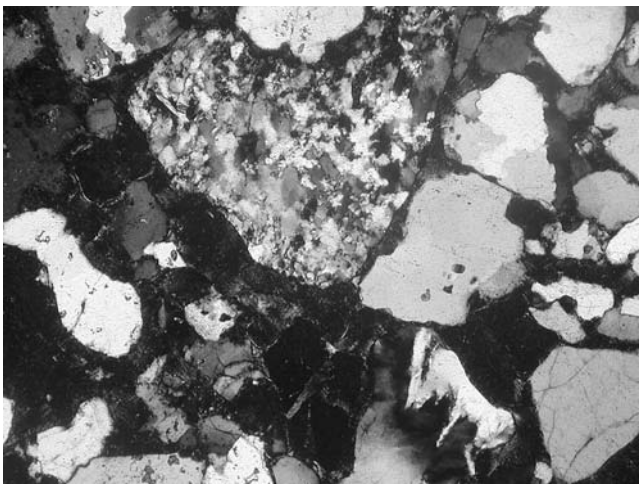

Fig. 2 Microscopic character of the rock substrate on which efflorescence occur. The microphotograph was taken in crossed nicols, the longer side represents about 4 mm

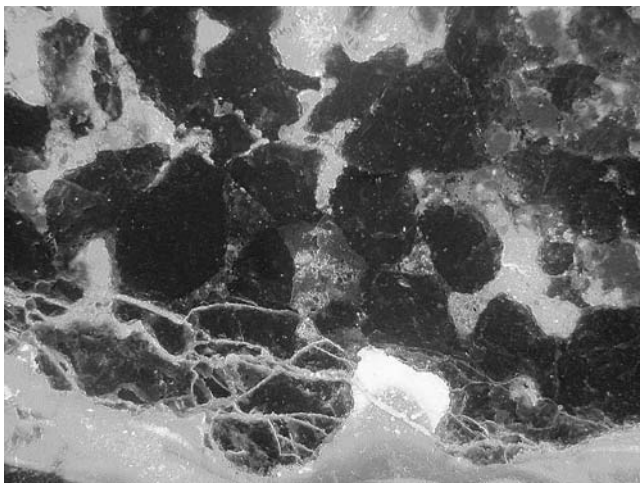

Fig. 3 The character of pore space (*bright areas*) in studied sandstones. Example of sample affected by granular disintegration where the surface case hardening is absent and exfoliation microcracks parallel to the exposed surface are developed at the bottom of the image. The reflected ultraviolet light mode, the longer side of the image represents about 2 mm

inherited feature from older geological periods. Similar features can be found in Cretaceous sandstones within Bohemian Cretaceous Basin that are not affected by salt crystallisation.

Other mineral phases comprise muscovite, rutile and zircon that occur as the accessory phases. The matrix is composed by clay minerals (kaolinite). The secondary phases are represented by irregularly distributed Fe-oxihydroxides in matrix. Some samples show significant presence of secondary siliceous cement (Fig. 4) filling the pore space close to the exposed surface.

The pore system of the rock can be described as interclastic but in the surface layer, common transclastic microcracks (Fig. 3) parallel to the surface occur. These exfoliation features result either from temperature changes of insulated surfaces or due to crystallizing salts.

Phase and chemical composition of efflorescence

Sulphates prevail among the newly formed crystalline phases in studied efflorescence. Along with dominant potassium alum and gypsum (Table 2) other Al-rich sulphates like tschermigite, alunite and/or alunogen form common admixtures in most of the samples. Nitrammite and hydrophilite are less common non-sulphate phases. All these minerals can be considered as newly formed phases whilst common quartz represents the clastic phase liberated from rock substrate by the granular disintegration (driven by crystallisation of salts).

Because of the detection limit of XRD (about 2–4 wt%) and of its low capability to determine the content of cryptocrystalline or amorphous phases, the composition of water soluble extracts were studied by the IEC method (Table 3). This method confirmed the presence of dominant sulphate anions although nitrates are clearly detectable as well. Minor amounts of chlorides and phosphates can be observed in certain cases. The IEC method also allows detailed speciation of cations among which the most interesting is the relatively high content of magnesium. Interestingly, no crystalline phase containing magnesium was determined by XRD (Fig. 4).

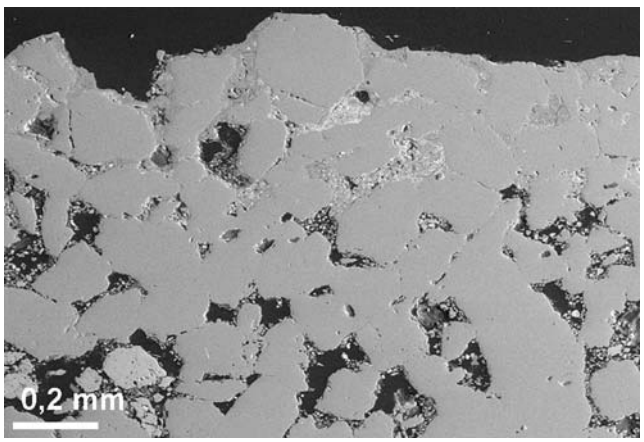

Fig. 4 SEM image of the sandstone where secondary silica cement completely engrosses the pore system and causes case hardening of the rock

Table 2 Phase composition of efflorescence as determined by XRD

Sample	Height above the ground (m)	Sulphates	Chlorides	Nitrates
North facing exposure				
KS/II/1a	0.5–0.6	Gypsum, potassium alum	ND	ND
KS/II/2a	1.0–1.1	Gypsum, potassium alum	ND	ND
KS/II/3a	2.0–2.2	Gypsum, potassium alum	ND	ND
KS/II/4a	2.5–2.6	Gypsum, potassium alum	Hydrophilite	ND
South facing exposure				
KS/IV/1a	0.35	Gypsum, potassium alum	ND	Nitrammite
KS/IV/2a	0.7	Gypsum, potassium alum	ND	Nitrammite
KS/IV/3a	1.1	Gypsum, potassium alum, mendozite	ND	ND
KS/IV/4a	1.5	Gypsum, potassium alum	ND	ND
KS/IV/5a	1.8–1.9	Gypsum, potassium alum, tschermigite	ND	ND
KS/IV/6a	2.1–2.2	Gypsum, potassium alum, tschermigite	ND	ND
East facing exposure				
KS/V/1a	0.4–0.5	Gypsum, potassium alum	Hydrophilite	ND
KS/V/2a	1.0–1.1	Gypsum, potassium alum	ND	Nitrammite
KS/V/3a	1.4	Gypsum, potassium alum	ND	Nitrammite
KS/V/4a	1.7	Gypsum, potassium alum, alunite, alunogen	ND	ND
KS/V/5a	1.8	Gypsum, potassium alum	ND	ND
KS/V/6a	2.1	Gypsum, potassium alum	ND	Nitrammite
KS/V/7a	5	Gypsum, potassium alum	ND	ND
KS/V/8a	6	Gypsum, potassium alum	Hydrophilite	Nitrammite
KS/V/9a	6	Gypsum, potassium alum, alunite	ND	ND
West facing exposure				
KS/VI/1a	0.7	Gypsum, potassium alum	Hydrophilite	Nitrammite
KS/VI/2a	1.2	Gypsum, Potassium alum, alunite	ND	ND
KS/VI/3a	1.5	Gypsum, potassium alum	hydrophilite	ND
KS/VI/4a	1.5–1.6	Gypsum, potassium alum	ND	Nitrammite
KS/VI/5a	2.0–2.1	Gypsum, potassium alum	ND	ND
North facing exposure				
KS/VII/1a	0.4	Gypsum, potassium alum	Hydrophilite	Nitrammite
KS/VII/2a	0.5	Gypsum, potassium alum, alunogen	ND	ND
KS/VII/3a	0.8	Gypsum, potassium alum	ND	ND
KS/VII/4a	1.0	Gypsum, potassium alum, alunite	Hydrophilite	ND
KS/VII/5a	1.6	Gypsum, potassium alum	ND	ND
KS/VII/6a	2.1	Gypsum, potassium alum	ND	ND

Potassium alum ($KAl(SO_4)_2{\cdot}12H_2O$), tschermigite ($NH_4Al(SO_4)_2{\cdot}12H_2O$), alunite ($K(Al_3(SO_4)_2(OH)_6)$), alunogen ($Al_2(SO_4)_3{\cdot}17H_2O$), gypsum ($CaSO_4{\cdot}2H_2O$), hydrophilite ($CaCl_2$), nitrammite ($NH_4\,NO_3$), mendozite ($NaAl(SO_4)_2\,12H_2O$)

Origin of salts

As shown by previous studies on isotopic composition of S and O from sulphates (Buzek and Šrámek 1985; Buzek et al. 1991; Novák et al. 2001; Přikryl and Soukupová 2001; Přikryl et al. 2004) the sulphur of salt efflorescences in the Czech Republic originates from atmospheric SO_2 due to the combustion of high-sulphur brown coal in NW Bohemia. The gypsum originates through the reaction of SO_2 with calcium anion that is probably derived also from the acid rain (Stumm and Morgan 1981) because the rock substrate–quartz sandstone with clay matrix is Ca^{2+} deficient. The other possible source of Ca^{2+} can be ground water (Winkler 1994) or the particulate matter in the atmosphere (Rodriguez-Navarro and Sebastian 1996). Other sources of sulphur, namely sulphide oxidation (e.g. Joeckel et al. 2005) can be excluded due to a completely different stable isotope ($\delta^{34}S$ and $\delta^{18}O$) pattern of the efflorescence from the same area (Přikryl and Soukupová 2001).

Efflorescence on Cretaceous sandstones from NW Bohemia is characterised by a high content of Al-rich sulphates as shown by this and previous studies (Beyer 1911; Breiter 1976; Soukupová et al. 2002). These minerals can be formed in two steps. During the first step, K^+, Na^+ and Ca^{2+} rich sulphates are formed due to the release of the above mentioned anions from feldspars and clay minerals. When all alkalis are scavenged by the reaction, Al^{3+} anions are released from decomposed feldspars and/or clay minerals followed by the formation of alunogen. Occurrence of this phase

Table 3 Concentration of anions and cations of water-soluble salts in studied rocks as determined by IEC method

Sample	Height above the ground (m)	Cl^-	F^-	NO_2^-	NO_3^-	PO_4^{3-}	SO_4^{2-}	Ca^{2+}	K^+	Mg^{2+}	Na^+	NH_4^+
North facing exposure												
KS/I/1	0.5	0.01	b.d.l.	b.d.l.	0.03	b.d.l.	0.33	0.01	0.02	0.01	0.01	0.01
KS/I/2	1.0	0.01	b.d.l.	b.d.l.	0.04	b.d.l.	0.62	0.03	0.03	0.01	0.02	0.01
KS/I/3	1.5	0.01	b.d.l.	b.d.l.	0.02	0.01	0.60	b.d.l.	0.05	0.01	0.01	0.01
KS/I/4	2.0	b.d.l.	b.d.l.	b.d.l.	0.01	b.d.l.	0.49	0.03	0.05	b.d.l.	0.01	0.02
KS/I/5	2.5	b.d.l.	b.d.l.	b.d.l.	b.d.l.	b.d.l.	0.06	0.02	b.d.l.	b.d.l.	b.d.l.	b.d.l.
South facing exposure												
KS/IV/1	0.35	0.02	b.d.l.	b.d.l.	0.03	b.d.l.	0.37	0.01	0.01	0.06	0.08	b.d.l.
KS/IV/2	0.7	0.01	b.d.l.	b.d.l.	0.11	0.02	0.44	0.03	0.02	0.04	0.05	0.01
KS/IV/3	1.1	0.01	b.d.l.	b.d.l.	0.20	0.01	0.63	0.01	0.07	0.06	0.06	0.02
KS/IV/4–1	1.6	0.01	b.d.l.	b.d.l.	0.13	b.d.l.	0.54	b.d.l.	0.03	0.06	0.05	0.02
KS/IV/5	1.9	0.01	b.d.l.	b.d.l.	0.12	b.d.l.	0.80	b.d.l.	0.1	0.04	0.04	0.04
East facing exposure												
KS/V/1	0.5	b.d.l.	b.d.l.	b.d.l.	0.05	0.01	0.87	0.03	0.06	0.01	0.01	0.04
KS/V/2	1.0	b.d.l.	b.d.l.	b.d.l.	0.03	b.d.l.	0.31	0.01	0.02	0.01	0.01	0.01
KS/V/3	1.5	b.d.l.	b.d.l.	b.d.l.	0.01	b.d.l.	0.15	b.d.l.	b.d.l.	b.d.l.	0.01	b.d.l.
KS/V/4	2.0	b.d.l.	b.d.l.	b.d.l.	0.02	b.d.l.	0.8	0.05	0.07	b.d.l.	0.01	0.05
West facing exposure												
KS/VI/1	0.5	b.d.l.	b.d.l.	b.d.l.	0.01	0.01	0.75	0.03	0.03	0.01	0.01	0.03
KS/VI/2	1.0	b.d.l.	b.d.l.	b.d.l.	0.02	b.d.l.	0.60	0.05	0.03	0.01	0.01	0.02
KS/VI/3	1.55	b.d.l.	b.d.l.	b.d.l.	0.05	b.d.l.	1.05	0.05	0.08	0.01	0.02	0.04
KS/VI/4	2.0	b.d.l.	b.d.l.	b.d.l.	0.01	b.d.l.	0.49	0.07	0.02	b.d.l.	0.01	0.01
KS/VI/5	2.5	0.01	b.d.l.	b.d.l.	0.09	b.d.l.	0.51	0.05	0.03	b.d.l.	0.01	0.01

Data are presented in wt%, b.d.l. below detection limit

can indicate either the depletion of neutralisation capacity of soils and rocks substrate or lower washing out of the salts due to the drier and warmer climate.

The high sulphur content in rainwater is a consequence of atmospheric pollution in north and northwest Bohemia which has been historically influenced by an enormous release of SO_2 due to the combustion of brown coal with high sulphur content. The mineralogical composition of efflorescence (above all the presence of Al-rich sulphates on natural sandstone outcrops) is predetermined by the chemical composition and the acid character of precipitation.

Regular monitoring of chemical composition of air and precipitation started in the area of the Bohemian Switzerland National Park in 2002. During last five years, the sulphur content slowly declined but still remains in the range of 2.0–3.15 mg/l (Fig. 5) but average annual pH of precipitation still fluctuates from 4 to 5 during last 4 years and exhibits decreasing trend (Fig. 5). This is probably caused by an increasing amount of NO_x in the atmosphere. The behaviour of aluminous phases in acid conditions is based on ''theoretical'' gibbsite (aluminium hydroxide) which dissolves more rapidly under pH below 6 (Drever 1988). It has been also confirmed experimentally that aluminous phases decompose faster in the presence of sulphates (Ridley et al. 1997). The dominant potassium alum indicates the possibility of feldspar decomposition and release of potassium. K^+ makes a common admixture in NH_4^+/Al^{3+} structures where K^+ mobility increases with a decreasing molar ratio of NH_4^+/Al^{3+} in solution (Hostomský et al. 1998).

Along with sulphates, some minor admixtures of chlorides and nitrates were detected by XRD and IEC. The XRD allows identification of two phases: hydrophilite and nitrammite. These two phases, are not, however, the sole combination of Cl^- or NO_3^- anions with present cations. Based on the IEC data, the presence of thenardite (Na_2SO_4) cannot be excluded although not confirmed by XRD. Nitrates, chlorides and NH_4^+ make common admixtures in acid precipitation (Stumm and Morgan 1981). Nitrates and NH_4^+ can originate from the soil and biosphere. The fertilizers can be excluded due to the location of the studied area in the strictly protected part of the national park where any agricultural activity is prohibited.

Directional factors influencing salt distribution

The salt distribution in the studied area exhibits directional dependence that can be expressed by two factors: the geographic orientation of studied profiles and position of the sampling point above the ground (height dependence). The vertical profiles of salt distribution on Wing Wall cliffs do not correspond precisely to the previously published models proposed for buildings and monuments (e.g., Arnold and Zehnder 1990). According to this model, the dominant crystallisation height of salts in a 0.5–1 m interval correlates with the maximum damage of substrate material.

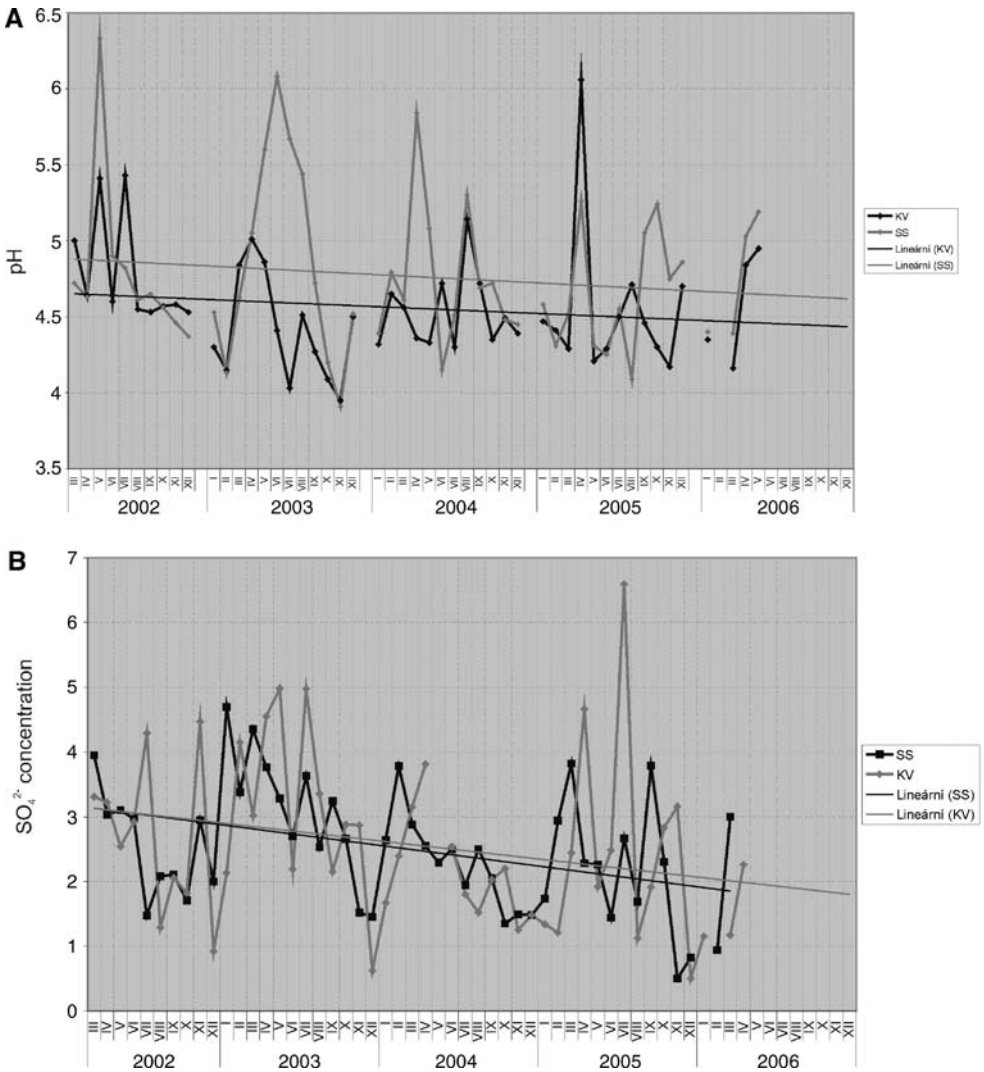

Fig. 5 Measured pH value and sulphate content in precipitation on the monitored locality called Silver Walls (Stříbrné stěny) cliffs (SS, 3 km distant from the Wing Walls cliffs) and Marten hill (Kuní vrch, KV) in the central part of the National Park Bohemian Switzerland area

The studied profiles on a natural exposure show two zones with maximum salt distribution and maximum damage of the rock on south and east exposures and one zone on north and west exposures. On the south exposure, the maximum salt concentration was detected in the height of 1and 2 m, for the east exposure in the height of 0.5 and 2 m (Table 3). The lower maximum is probably due to the raising damp rising from the ground. The second maximum in about 2 m represents salt accumulated from the washed overlying rock profile from descending precipitation. The south exposure shows first maximum of salt concentration at about 1 m above the ground where both sulphates and nitrates occur. The second maximum at about 2 m is manifested by higher contents of sulphates. For the west exposure, the maximum concentration of sulphate anion occurs at about 1.5 m above the ground whilst nitrates are shifted to about 2.5 m. The north exposure shows a corresponding maximum concentration of sulphates and nitrates at the 1–1.5 m interval.

The observed data thus do not confirm the model of salt movement due to damp rising and stratification of sulphates in lower parts and nitrates in higher parts of the wall (Arnold and Zehnder 1990). The measured data more likely indicate the multiple sources of some anions or cations that contribute to the salt weathering on analysed cliffs. The first source can be considered, without any doubt, from the polluted atmosphere and from precipitation. These compounds are introduced by the precipitation that percolates through the porous sandstone just to the base of the cliffs where they evaporate. A second source of salts can be found in the ground or in rocks lying below the ground. The salts can be present either due to a previous accumulation or can be transported from the ground water.

Changes of physical properties

Although the studied rock shows uniform fabric (namely grain size of present clasts) over the analy-

Table 4 Physical properties of studied rocks

Sample	Height above the ground (m)	Moisture content (wt %)	Water absorption (wt %)	Bulk porosity (vol. %)	Capillary porosity (vol. %)	Radii moduses of capillary pores (nm)	Percentage of capillary pores from the bulk porosity (%)
North facing exposure							
KS/I/1	0.5	4.7	14.0	43.9	5.2	1,881	11.8
KS/I/2	1.0	3.3	12.2	39.2	4.9	230	12.5
KS/I/3	1.5	3.6	10.1	36.8	3.5	109	9.5
KS/I/4	2.0	3.6	10.2	34.0	3.3	751	9.7
KS/I/5	2.5	5.7	12.9	25.6	ND	ND	ND
South facing exposure							
KS/IV/1	0.35	5.3	9.6	37.5	ND	ND	ND
KS/IV/2	0.7	4.3	10.4	16.3	5.8	260	35.6
KS/IV/3	1.1	10.5	10.7	32.6	6.6	3,205	20.3
KS/IV/4–1	1.6	6.8	2.4	26.9	ND	ND	ND
KS/IV/5	1.9	8.0	11.0	40.6	3.0	3,503	7.4
East facing exposure							
KS/V/1	0.5	5.7	6.3	37.1	4.0	249	10.8
KS/V/2	1.1	14.1	8.5	29.1	3.5	225	12.0
KS/V/3	1.5	7.6	9.0	31.4	5.3	236	16.9
KS/V/4	2.0	2.8	10.2	28.7	ND	ND	ND
West facing exposure							
KS/VI/1	0.5	4.8	4.3	33.2	4.5	244	13.6
KS/VI/2	1.0	9.4	9.5	39.0	3.5	114	9.0
KS/VI/3	1.55	8.5	9.3	34.5	3.8	236	11.0
KS/VI/4	2.0	4.5	7.8	31.8	ND	ND	ND
KS/VI/5	2.5	7.0	8.7	34.0	8.6	1,364	25.3

sed profile, they are characterised by a significant variation of physical properties like porosity and water absorption (Table 4). Porosity is a significant petrophysical parameter that expresses the physical state of the rock but is also part of the rock fabric (Přikryl 2006). For sedimentary rocks showing uniform size distribution of clasts one should expect uniform size distribution of pores as well. However, porosity can be significantly modified by crystallizing salts (Goudie 1999) among which K/NH_4–Al sulphates are considered to be the most destructive (Williams and Robinson 1998). The freeze/thaw cycle contributes to the increase of porosity, too (Thomachot and Jeannette 2002). Higher porosity causes deterioration of rock mechanical properties, namely tensile and compressive strength (e.g., Goodman 1989) and thus speeds up granular disintegration of the rock.

The studied rocks exhibited higher porosity in places with higher concentrations of water-soluble salts (namely of sulphates and nitrates). The increase of porosity is considered to be due to the weathering process. Simultaneously, higher porosity means larger volumes of water that can be absorbed into the pore system (here expressed by measurement of natural moisture content or by water absorption).

Along with bulk porosity, the important information on the physical changes in the rock fabric due to the crystallizing salts and/or freezing/thawing of the water can be derived from detailed pore fabric analysis (mean pore size and volume of pores of variable size). The mercury porosimetry data show that volume of macropores and mesopores (following IUPAC terminology) increases with the increasing content of water-soluble salts. The measurement also confirmed that a higher concentration of salts is accompanied by the opening of pores and shift of mean pore size from several hundreds to the first thousand nm (Table 4).

The changes in the pore system caused by the weathering were also studied by optical microscopy. The optical microscopy in the UV reflected light mode confirmed increase of pore volume and decrease of cohesion of clasts in surface layer due the crystallisation of salts. Moreover, some clasts close to the exposed surface are disturbed by common exfoliation microcracks (see Fig. 3). These microcracks evidently facilitate water percolation through the rock and accelerate disintegration of the rock.

Conclusions

The studied sandstone exposed on the Wing Wall cliffs (National Park Bohemian Switzerland, northwest Bohemia, Czech Republic) shows extensive modification of rock fabric and deterioration of physical properties due to crystallising salts and/or freezing/thawing of water in pores. The weathering of sandstone is macroscopically manifested on case hardened surfaces, by efflorescence/subflorescence, followed by uneven granular disintegration and formation of micro- to macrorelief (e.g., honeycombs).

The salts are formed by dominant, newly formed sulphates, and minor chlorides (hydrophilite) and nitrates (nitrammite) as determined by XRD. Along with the most common phases, gypsum and potassium alum, some other Al-rich sulphates (tschermigite, alunite, alunogen) occur as well. Because of the detection limit of XRD, the composition of water-soluble salts was also interpreted from chemical analysis performed by ion exchange chromatography. The IEC allows a precise speciation of anions and cations although it does not provide a possibility to detect mineral phases. Based on the chemical data, the presence of some other phases is expected (namely thenardite) although not confirmed by XRD.

The occurrence of specific species is influenced by geographic factors and by the solubility of salts. More soluble phases occur in sheltered areas not directly exposed to atmospheric agents (shelters, cavities) and on the geographic orientation where lower elution or higher insulation can be expected. The most soluble phases (hydrophilite, nitrammite and tschermigite) crystallise on the surface exposed to the south. Soluble salts can be present, however, on the surface exposed to the east and west, too. The surface oriented to the north is characterised by less soluble gypsum and potassium alum.

The specific mineralogical and chemical composition of the studied efflorescence is influenced by both the mineralogical composition of the rock (presence of feldspars and clay minerals) and by atmospheric pollution of the area. The acidity of precipitation (pH from 4 to 5) facilitates release of alkalis and aluminum from rock-forming minerals (namely from feldspars but probably also from clay minerals). The presence of SO_2 in the atmospheric deposition contributes to the formation sulphates.

The distribution of salts varies directionally: both according to the geographic orientation of studied profiles and to the height of the sampling point. On the morphologically indented surfaces, two maxima of salt distribution occur in the 0.5–1 m and 2–2.5 m above the ground. The presence of specific salts is thus influenced by both rising moisture (the lower exposed maximum) from the ground and by the percolation of the precipitation (the higher exposed maximum) through the rock mass from the higher altitudes.

Modification of rock fabric (namely opening of smaller pores) due to the weathering and associated deterioration of physical properties positively correspond to the concentration of water-soluble salts. The physical changes become evident mainly by increasing water absorption and bulk porosity. Increase of bulk porosity is dominant in the surface layer followed by decreasing cohesion of the clasts and higher susceptibility to the granular disintegration. The change of pore system is accompanied by extensive formation of exfoliation microcracks in clasts present in the surface layer.

Acknowledgments The cooperation of the Management Authority of the National Park Bohemian Switzerland is highly appreciated for making it the possible to collect samples in the protected zone of the park. Petr Drahota (Institute of Geochemistry, Mineralogy and Mineral Resources, Charles University) kindly measured raw XRD data. The financial support for this research came from the MSM 113100005 project. The porosity study was made possible through the A3046401 project (Grant Agency of the Academy of Sciences of the Czech Republic). Z. Vařilová appreciated institutional financial support from the Institute of Geology, Academy of Sciences of the Czech Republic (Project No. AV0Z30130516). John Novotney kindly helped with the English checking of the final version of this paper.

References

Adamson AW (1967) Physical chemistry of surfaces. Interscience, New York

Arnold A (1982) Rising damp and saline minerals. In: Gauri KL, Gwinn (eds) Fourth international congress on the deterioration and preservation of stone objects. Louisville, Kentucky, pp 11–28

Arnold A, Zehnder K (1990) Salt weathering on monuments. Advanced workshop analytical methodologies for the investigation of damaged stone, September 14–21, 1990. Pavia, Italy, 58 pp

Behlen A, Steiger M, Dannecker W (1997) Quantification of the salt input by wet and dry deposition on a vertical masonry. In: Moroupoulou A (ed) Fourth international symposium on the conservation of monuments in the mediterranean basin. Technical Chamber of Greece, Rhodes, pp 237–246

Beyer O (1911) Alum and gypsum as new formed minerals and causes of chemical weathering in thick-bedded sandstones of Saxonian Cretaceous formation. Z Dt Geol Ges 63:429–467

Breiter K (1976) Occurrence of sulphates on Upper Cretaceous thick-bedded sandstones in north Bohemia (in Czech). Sborn Severočes Mus Ser Natur 8:99–107

Buzek F, Šrámek J (1985) Sulfur isotopes in the study of stone monument conservation. Stud Conserv 30:171–176

Buzek F, Černý J, Šrámek J (1991) Sulphur isotope studies of atmospheric S and the corrosion of monuments in Prague,

Czechoslovakia. In: Krouse HR, Grinenko VA (eds) Stable isotopes, natural and anthropogenic sulphur in the environment, SCOPE 43. Wiley, Chichester, pp 399–405
Camuffo D, Del Monte M, Sabbioni C (1983) Origin and growth mechanisms of the sulfated crusts on urban limestone. Water Air Soil Pollut 19:351–359
Charola AE (2000) Salts in the deterioration of porous material: an overview. J Am Inst Conserv 39:327–343
Cortecci G, Longinelli A (1970) Isotopic composition of sulfate in rain water, Pisa, Italy. Earth Planet Sci Lett 8:36–40
Drever JI (1988) The geochemistry of natural waters. Prentice-Hall, London
Engel Z, Kalvoda J (2002) Morphostructural development of the sandstone relief in the Bohemian Cretaceous Basin. In: Přikryl R, Viles HA (eds) Understanding and managing stone decay. Karolinum, Praha, pp 225–231
Goodman RE (1989) Introduction to rock mechanics. Wiley, New York
Goudie A (1999) Experimental salt weathering of limestones in relation to rock properties. Earth Surf Process Landf 24:715–724
Goudie A, Viles H (1997) Salt weathering hazards. Wiley, Chichester
Hostomský J, Hostomská V, Bezdička P, Selucká J (1998) Phase equilibria during the crystallisation of ammonium alum from acid solutions with a variable ratio NH_4/Al (in Czech). Unpublished report of the Institute of Chemical Technology in Prague
JCPDS (1999) Powder diffraction file, PDF-2, international centre for diffraction data, Newtown, Pennsylvania
Joeckel RM, Clement BJA, Bates LRVF (2005) Sulfate-mineral crusts from pyrite weathering and acid rock drainage in the Dakota formation and Graneros Shale, Jefferson County. Nebraska Chem Geol 215:433–452
Machill S, Althaus K, Krumbein WE, Steger WE (1997) Identification of organic compounds extracted from black weathered surfaces of Saxonean sandstones, correlation with atmospheric input and rock inhabiting microflora. Org Geochem 27:79–97
Magee AW, Bull PA, Goudie AS (1988) Chemical textures on quartz grains and experimental approach using salts. Earth Surf Process Landf 13:665–676
Marsh H, Rodríguez-Reinoso F (2000) Science of carbon materials. Publicaciones de la Universidad de Alicante, Alicante
McAlister JJ (1996) Analytical techniques for the examination of building stone. In: Smith BJ, Warke PA (eds) Processes of urban stone decay. Donhead, London, pp 171–193
Nishiyama T, Kusuda H (1994) Identification of pore spaces and microcracks using fluorescent resins. Int J Rock Mech Min Sci Geomech Abstr 31:369–375
Novák M, Jačková I, Přechová E (2001) Temporal trends in the isotope signature of air-borne sulfur in Central Europe. Environ Sci Technol 35:255–260
Price JE (1990) Geology of construction materials. Chapman & Hall, London
Price CA (1996) Stone conservation. The Getty Conservation Institute, Santa Monica
Přikryl R (2006) Assessment of rock geomechanical quality by quantitative rock fabric coefficients: Limitations and possible source of misinterpretations. Eng Geol 87:149–162
Přikryl R (2007) Understanding the earth scientist's role in the pre-restoration research of monuments: an overview. In: Přikryl R, Smith BJ (eds) Building stone decay: from diagnosis to conservation. Geological Society London, Special Publications, 271:9–21
Přikryl R, Soukupová J (2001) Research on mechanisms of the weathering crust formation on sedimentary rocks exposed in natural and polluted environments. Unpublished report to the Ministry of Environment of the Czech Republic, p 21
Přikryl R, Svobodová J, Žák K, Hradil D (2004) Anthropogenic origin of salt efflorescences on sandstone sculptures (Charles bridge, Prague, Czech Republic)—mineralogical and stable isotope geochemistry evidence. Eur J Mineral 16:609–617
Pye K, Schiavon N (1989) Cause of sulphate attack on concrete, render and stone indicated by sulphur isotope ratio. Nature 342:663–664
Ridley MK, Wesolowski DJ, Palmer DA, Bénézeth P, Kettler RM (1997) Effect of sulphate on the release rate of Al^{3+} from gibbsite in low-temperature acidic waters. Environ Sci Technol 31:1922–1925
Rodriguez-Navarro C, Doehne E (1999) Salt weathering: influence of evaporation rate, supersaturation and crystallization pattern. Earth Surf Process Landf 24:191–209
Rodriguez-Navarro C, Doehne E, Sebastian E (1999) Origins of honeycomb weathering: The role of salt and wind. Geol Soc Am Bull 111:1250–1255
Rodriguez-Navarro C, Sebastian E (1996) Role of particule matter from vehicle exhaust on porous building stones (limestone) sulphation. Sci Total Environ 187:79–91
Smith BJ, Turkington AV, Curran JM (2001) Calcium loading of quartz sandstones during construction: Implications for future decay. Earth Surf Process Landf 26:877–883
Schweigstillová J, Novotná M, Přikryl R (in prep) Chemical and isotopic composition of salt efflorescence from the sandstone castellated rocks of the Bohemian Cretaceous Basin (Czech Republic) (submitted to Environ Geol)
Soukupová J, Hradil D, Přikryl R (2002) Chemical weathering of clay-rich sandstone matrix—control and case studies. In: Přikryl R, Viles HA (eds) Understanding and managing stone decay. Karolinum, Praha, pp 263–271
Steiger M (1996) Distribution of salt mixtures in a sandstone monument: sources, transport and crystallization properties. In: Zezza F (ed) EC research workshop on origin, mechanisms and effects of salts on degradation of monuments in marine and continental environments. Protection and conservation of European cultural heritage, research report 4, Bari, pp 241–246
Steiger M, Behlen A, Neumann HH, Willers U, Wittenburg C (1997) Sea salt in historic buildings: deposition, transport, accumulation. In: Moroupoulou A (eds) Fourth international symposium on the conservation of monuments in the Mediterranean Basin. Technical Chamber of Greece, Rhodes
Stumm W, Morgan JJ (1981) Aquatic chemistry. Willey, New York
Thomachot C, Jeannette D (2002) Evolution of the petropyhsical properties of two types of Alsatian sandstone subjected to simulated freeze-thaw conditions. In: Siegesmund S, Weiss T, Vollbrecht A (eds) Natural stone, weathering phenomena, conservation strategies and case studies. Geological Society, London, Special Publications 205:19–32
Torfs KM, van Grieken RE, Buzek F (1997) Use of stable isotope measurements to evaluate the origin of sulphur in gypsum layers on limestone building. Environ Sci Technol 31:2650–2655
Vařilová Z (2002) A review of selected sandstone weathering forms in the Bohemian Switzerland National Park, Czech Republic In: Přikryl R, Viles HA (eds) Understanding and managing stone decay. Karolinum, Praha, pp 233–242

Williams RBG, Robinson DA (1998) Weathering of sandstone by alunogen and alum salts. Q J Eng Geol 31:369–373

Winkler EM (1994) Stone in architecture—properties, durability. Springer, Berlin Heidelberg New York

Young ARM (1987) Salt as an agent in the development of cavernous weathering. Geology 15:962–966

Zehnder K (1993) New aspects of decay caused by crystallization of gypsum. In: Thiel MJ (ed) Conservation of stone and other materials. Causes of disorders and diagnosis, vol. 1. E&FN Spon, London, pp 107–114

Zehnder K (1996) Gypsum eflorescence in the zone of rising damp. Monitoring of slow decay processes caused by crystallizing salts on wall paintings. In: Riederer J (ed) Proceedings of eighth international congress on deterioration and conservation of stone. Ernst und Sohn, Berlin, pp 1669–1678

Zvelebil J, Cílek V, Stemberk J (2002) Partial results of monitoring of stability deterioration on Pravčice Rock Arch, NW Bohemia. In: Přikryl R, Viles HA (eds) Understanding and managing stone decay. Karolinum, Praha, pp 243–261